

# Giant Magnetostrictive Materials for Field Weakening: A Modeling Approach

Guillaume Krebs<sup>1</sup> and Laurent Daniel<sup>1,2</sup>

<sup>1</sup>Laboratoire de Génie Electrique de Paris (LGEPE), SUPELEC, CNRS (UMR 8507), UPMC, Univ Paris-Sud, 91192 Gif-sur-Yvette Cedex, France

<sup>2</sup>Materials Science Centre, University of Manchester, Manchester M1 7HS, U.K.

In this paper, a proposal for a field weakening method for a permanent-magnet synchronous motor is evaluated. The method consists in inserting giant magnetostrictive elements between permanent magnets. The magnetic permeability of these magnetostrictive parts is modified when the speed increases. The field leakages around the permanent magnets are consequently increased, thus reducing the electromotive forces in the armature windings. An original modeling approach, based on the concept of equivalent stress, is proposed in order to evaluate this field weakening solution.

**Index Terms**—Finite element methods, magnetoelasticity, permanent-magnet motors.

## I. INTRODUCTION

IN electrical or hybrid automotive applications, torque and power features usually have the typical behavior shown in Fig. 1. For such applications, the use of permanent-magnet synchronous motor (PMSM) provides substantial advantages. In addition to rare earth magnets, they generally have reduced losses, a good torque/volume ratio, and are relatively easy to manufacture.

However, since the excitation field created by the permanent magnet (PM) is almost constant, a main drawback is the level of the electromotive forces (EMF) induced in the stator windings. Due to the maximum speed (typically between 10 000 to 30 000 rpm) and to the number of Ampere-turns necessary to produce the rated torque, the inverter output voltage is rapidly reached. Consequently, a compensation of the magnetic field created by the magnets is needed.

Several approaches have been proposed and applied. The most used is to control the magnitude and phase (d-q vectors) of the stator current and voltage. Another solution is to redirect the flux created by the magnets. However, an additional power is required in both cases. Field weakening operations can also be performed without power consumption. Mechanical devices (located either in the stator or in the rotor) can be used to redirect the magnetic field in the motor or to short-circuit the magnets. Nevertheless, the use of mobile parts can reduce the lifetime of the motor.

Magnets of PMSM are sometimes segmented in order to increase the flux weakening range. Based on this concept, we propose in this paper to fill the gap between the magnets with parts made of giant magnetostrictive material (GMM). The material and the location of these parts are chosen in such a way that the magnetic permeability varies with the inertial stress due to the

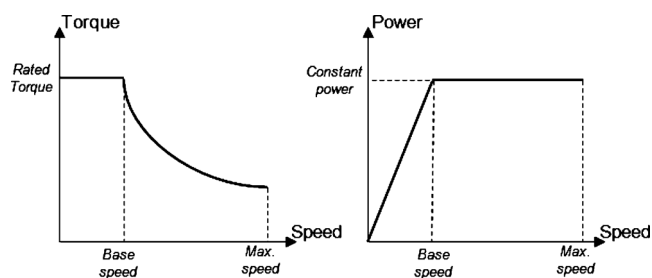


Fig. 1. Typical torque and power behavior in automotive application.

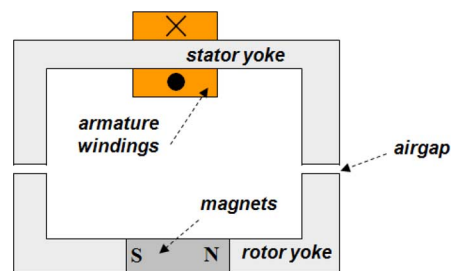


Fig. 2. Simplified representation of a PMSM [4].

rotation speed. Then no additional power and moving parts in the rotor are required for the field weakening.

In the first part of the paper, an overview of the classical flux and field weakening methods is proposed to highlight the potentiality of weakening methods based on the use of GMM. In the second part, a 2-D magnetomechanical model requisite for the modeling of these latter methods is presented. This modeling scheme is finally applied to a PMSM, confirming the relevance of the use of GMM for field weakening.

## II. FLUX AND FIELD WEAKENING METHODS

Various weakening approaches have been proposed and discussed in the literature [1]–[3]. They can be classified with respect to the amount of energy required to perform the EMF reduction. For the sake of simplicity, the following discussion will be based on a generic representation of PMSM presented in Fig. 2.

Manuscript received September 22, 2011; revised February 29, 2012; accepted April 05, 2012. Date of publication April 25, 2012; date of current version August 21, 2012. Corresponding author: G. Krebs (e-mail: guillaume.krebs@lgepe.supelec.fr).

Color versions of one or more of the figures in this paper are available online at <http://ieeexplore.ieee.org>.

Digital Object Identifier 10.1109/TMAG.2012.2196283

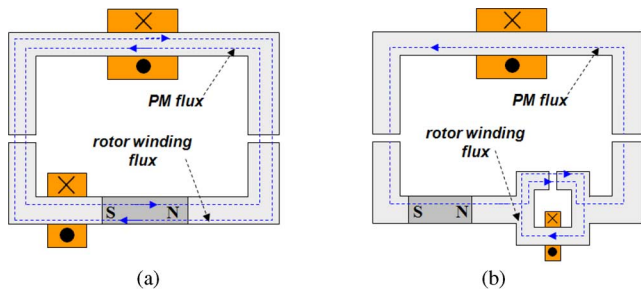


Fig. 3. Flux (a) and field (b) weakening solutions.

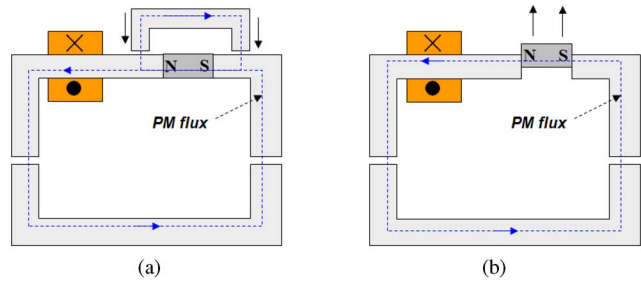


Fig. 4. Short-circuit (a) and shifting (b) of the PM.

#### A. Methods With Significant Additional Power Consumption

The most common method is the flux weakening approach. It consists in controlling the stator currents and voltages (in terms of phase and magnitude) in order to create in the air gap a field component opposite to the PM field. The currents and voltages are expressed in d-q reference system [5]. By controlling the q-axis current, the torque can be adjusted. The control of d-axis allows a reduction of the EMF.

The flux through the stator can also be reduced by the use of stator or rotor windings in addition to the magnets [6]; see Fig. 3(a).

Another example of field weakening makes use of an external coil powered in DC current to redirect the flux created by the magnets [7]. The flux circulation is then reduced and consequently the EMF; see Fig. 3(b).

However, these approaches can lead to supplementary losses and can demagnetize the magnets.

#### B. Methods With Minor Additional Power Consumption

Field weakening methods with minor additional consumption have also been proposed to reduce the EMF [8], [9].

The rotor and all its components can be moved out of the stator to reduce the magnetic active part. Another possibility applied to axial flux motors is to increase the air-gap length. Nevertheless, when operating conditions are severe (e.g., vibrations, temperature...), guiding and mechanical adjustment constraints can prohibit these methods.

In [10], the weakening of the EMF is performed using an external yoke that creates a magnetic short-circuit; see Fig. 4(a). This operation can be performed easily and efficiently if the magnets are located in the stator. The field circulation can also be modified by shifting the magnets out of the stator; see Fig. 4(b).

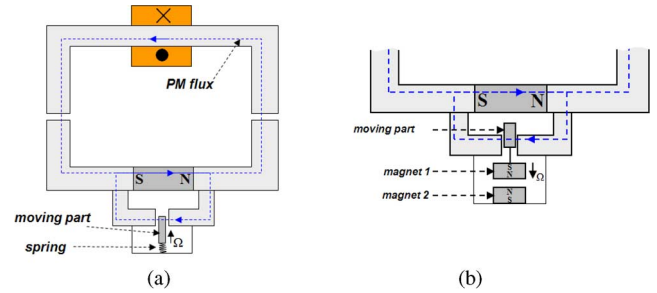


Fig. 5. Short-circuit moving parts with mechanical (spring) (a) or magnetic (magnets) (b) releasing system.

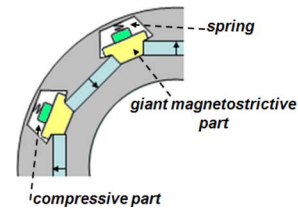


Fig. 6. Principle of a field weakening method using GMM [12].

These latter methods are easier to implement because the field weakening apparatus is positioned on a motionless part. But the use of actuators to perform the movement of this apparatus can increase the cost of the converter and the design complexity.

#### C. Methods Without Additional Power Consumption

Field weakening solutions without additional power consumption are particularly attractive for embedded systems or for high speed applications. Most of the solutions proposed in the literature use centrifugal effects. In order to create a magnetic short-circuit, moving ferromagnetic parts can be inserted; see Fig. 5(a). The motion of these additional parts is caused by the centrifugal forces. A spring is used to push the magnet back when speed decreases.

The spring can also be replaced by two magnets with opposite magnetization [11]; see Fig. 5(b). One of the magnets is connected to the moving part and its position depends on speed. However, the use of mobile parts inside the rotor can reduce the lifetime of the structure, notably due to wear issues.

#### D. GMM-Based Methods

The structure presented in [12] partially overcomes this drawback using giant magnetostrictive material (GMM). The principle of the structure is illustrated in Fig. 6.

The principle is based on the heavy stress dependence of the permeability of magnetic materials [13]–[15]. As an example, Fig. 7 shows the magnetic behavior of Terfenol-D under uniaxial compression stress.

At low speed, the spring exerts a compression stress on the GMM. The permeability is then low and there is very little leakage through the GMM. For higher rotation speed, the compression stress is reduced due to centrifugal forces. Thus, the permeability of the GMM increases and the EMF are reduced. For such a solution no moving part is introduced inside the rotor.

We propose to study the structure presented in Fig. 8. It is an interior permanent magnet motor with concentrated coils.

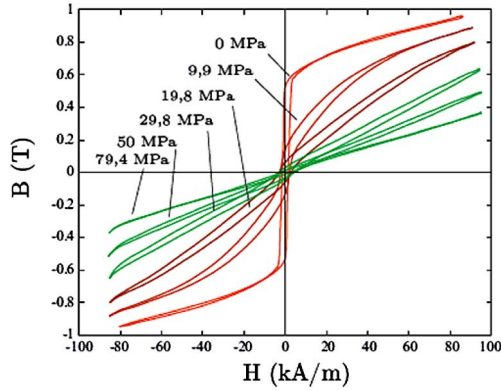


Fig. 7. Magnetic behavior of Terfenol-D under uniaxial compression stress [16].

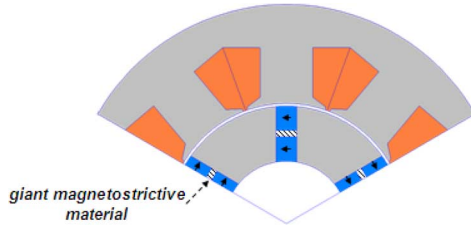


Fig. 8. Proposed PMSM motor with GMM parts.

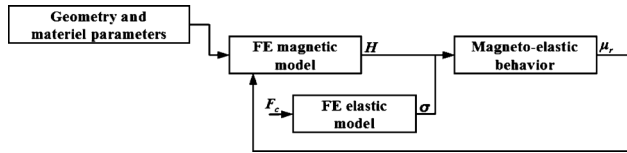


Fig. 9. Magnetoelastic calculation procedure.

GMM parts are inserted between the segmented magnets (hatched areas). This structure combines the interest of the flux weakening method using GMM together with the compactness of magnet flux concentration structures.

We suppose that a compressive stress is exerted on the GMM by the rotor poles. The technical realization of this loading is not handled in this paper—the use of encapsulated GMM could be suggested. The permeability of the GMM varies when the rotation speed increases. At high speed, the magnetic field from the magnets turns back through the GMM, reducing the stator EMF.

To study such a structure, a magnetoelastic problem has to be solved. The next section introduces the modeling tool proposed for that purpose.

### III. CALCULATION PROCEDURE

The calculation procedure is presented in Fig. 9.

First the problem is solved by means of a 2-D magnetic finite element (FE) formulation. The mechanical stress  $\sigma$  is obtained from a 2-D elastic FE formulation introducing the centrifugal forces  $\mathbf{F}_c$ . The values of  $\sigma$  and  $\mathbf{H}$  are then introduced as an input into the magnetoelastic constitutive law, defining a stress-dependent permeability. This permeability is introduced into the FE magnetic model. An iterative procedure is performed. We present hereafter the detail of each step of the process.

#### A. Magnetic Problem

We consider a domain  $\Omega$  with boundary  $\Gamma$  ( $\Gamma = \Gamma_B \cup \Gamma_H$  and  $\Gamma_B \cap \Gamma_H = \emptyset$ ). In the case of a linear magnetostatic problem, Maxwell's equations and constitutive law read

$$\text{div } \mathbf{B} = 0 \text{ with } \mathbf{b} \cdot \mathbf{n} = 0 \text{ on } \Gamma_B \quad (1)$$

$$\text{curl } \mathbf{H} = \mathbf{j} \text{ with } \mathbf{H} \times \mathbf{n} = 0 \text{ on } \Gamma_H \quad (2)$$

$$\mathbf{B} = \mu \mathbf{H}. \quad (3)$$

We can introduce the vector potential  $\mathbf{A}$  ( $\mathbf{B} = \text{curl } \mathbf{A}$ ) in the previous equation system. We obtain

$$\text{curl} \left( \frac{1}{\mu} \text{curl } \mathbf{A} \right) = \mathbf{j}. \quad (4)$$

In the 2-D case ( $\mathbf{B}$  defined on  $x$  and  $y$  axis for instance), only the  $z$  component of  $\mathbf{A}$  ( $A_z$ ) is expressed. Consequently, the previous expression becomes

$$\text{div} \left( \frac{1}{\mu} \text{grad } A_z \right) = j_z. \quad (5)$$

Weighted residual method is used with (5). The application of Green and Stokes theorems leads to (6). The eddy currents are neglected

$$\iint_{\Omega} \frac{1}{\mu} \text{grad}^t \psi \cdot \text{grad } A_z \, d\Omega = \iint_{\Omega} \psi j_z \, d\Omega. \quad (6)$$

The domain  $\Omega$  is meshed in order to solve (6) numerically. The vector potential  $A_z$  is approximated using the nodal element function. The system to solve is obtained using the Galerkin method where the test function  $\psi$  is chosen equal to the nodal element function.

The movement is taken into account using the locked step approach [17]. Local forces and global torque are calculated with the virtual work method.

#### B. Elastic Problem

The domain of study is  $\Omega$  of boundary  $\partial\Omega$ . Under static conditions, the equilibrium equation reads

$$-\text{div}(\sigma) = \mathbf{F} \text{ in } \Omega. \quad (7)$$

The boundary conditions are

$$\mathbf{u} = \mathbf{u}_0 \text{ on } \partial\Omega_u \quad (8)$$

$$\sigma_{ij} \mathbf{v}_j = \mathbf{f}_i \text{ on } \partial\Omega_f \quad (9)$$

$$(\partial\Omega = \partial\Omega_u \cup \partial\Omega_f \text{ and } \partial\Omega_u \cap \partial\Omega_f = \emptyset) \quad (10)$$

with  $\mathbf{u}$  the displacement vector,  $\sigma$  the stress tensor,  $\mathbf{F}$  the volume forces,  $\mathbf{f}$  the surface forces, and  $\mathbf{v}$  the direction normal to  $\partial\Omega$ . The strain tensor  $\varepsilon$  is defined by (11):

$$\varepsilon = \frac{1}{2}(\text{grad } \mathbf{u} + \text{grad}^t \mathbf{u}). \quad (11)$$

The stress tensor  $\boldsymbol{\sigma}$  is linked to the strain tensor  $\boldsymbol{\varepsilon}$  by the linear elastic constitutive law written as follows (using the Einstein summation convention):

$$\sigma_{ij} = \mathbf{C}_{ijkl} \varepsilon_{kl}. \quad (12)$$

The material is supposed to be homogeneous and elastically isotropic so that the constitutive law can be written using the two Lamé coefficients  $\lambda$  and  $\mu$ :

$$\boldsymbol{\sigma} = 2\mu\boldsymbol{\varepsilon} + \lambda \text{tr}(\boldsymbol{\varepsilon})\mathbf{1}. \quad (13)$$

The elastic problem can be expressed under the following form:

$$\int_{\Omega} \sigma_{ij} \varepsilon_{ij} dx = \int_{\Omega} \mathbf{F} \cdot \mathbf{v} dx + \int_{\partial\Omega} \mathbf{f} \cdot \mathbf{v} ds. \quad (14)$$

A 2-D configuration (plane strain assumption) is considered for the elastic problem.

### C. Magnetoelastic Behavior Modeling

In order to account for the effect of stress on the magnetic permeability of the GMM parts, a magnetoelastic constitutive law is needed. A classical way to characterize the magnetoelastic behavior of materials is to perform permeability measurements under tensile or compressive test (see for instance [16]). These experimental methods usually provide uniaxial characterizations that can be fitted and introduced into numerical simulations. However, in most electromagnetic devices, magnetic materials are submitted to multiaxial stress. A possible way to introduce the multiaxiality of stress into existing uniaxial magnetoelastic modeling tools is the definition of an equivalent stress criterion [18]. An equivalent stress for the magnetic behavior is a (fictive) uniaxial stress that would change the magnetic behavior in a similar manner than the (real) multiaxial one. Such an approach is classical in mechanics where Von Mises or Tresca equivalent stresses are used to define a plasticity criterion. In this paper, we will make use of a magnetoelastic equivalent stress proposed in [19], based on an equivalence in magnetoelastic energy. This equivalent stress  $\sigma^{\text{eq}}$  is defined by (15) using the Einstein summation convention:

$$\sigma^{\text{eq}} = \frac{3}{2} h_i s_{ij} h_j. \quad (15)$$

$\mathbf{h}$  is the magnetic field direction (unit vector) and  $\mathbf{s}$  is the deviatoric part of the stress tensor  $\boldsymbol{\sigma}$  defined by (16), where  $\delta_{ij}$  is the Kronecker symbol ( $\delta_{ij} = 1$  if  $i = j$  and  $\delta_{ij} = 0$  if  $i \neq j$ ):

$$s_{ij} = \sigma_{ij} - \frac{1}{3} \delta_{ij} \sigma_{kk}. \quad (16)$$

The implementation of such an equivalent stress can be made as follows. A model for magnetic behavior under uniaxial stress or corresponding experimental results are required. The stress state in the electromagnetic device is calculated first. An uncoupled

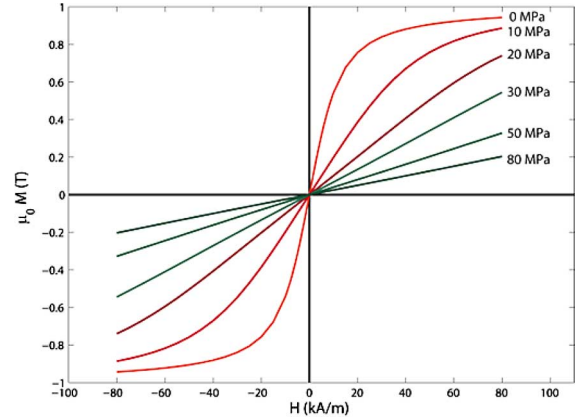


Fig. 10. Modeled magnetization curves.

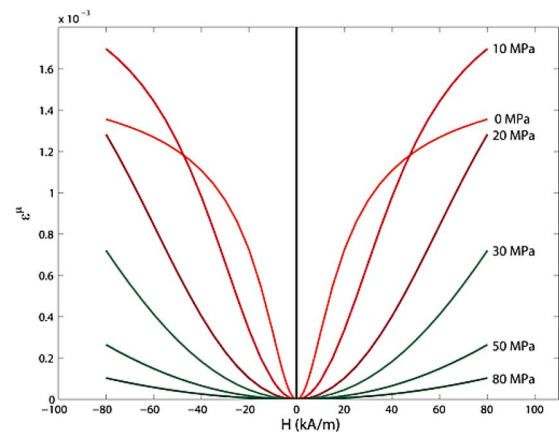


Fig. 11. Modeled magnetostriction curves.

magnetic calculation is done. The equivalent stress  $\sigma^{\text{eq}}$  is then calculated according to (15). The corresponding magnetic behavior of the material (e.g., permeability) is then deduced from the uniaxial model or experimental data in a configuration corresponding to a uniaxial stress of amplitude  $\sigma^{\text{eq}}$  applied in the direction parallel to the applied magnetic field. If the stress in the studied device depends on the magnetic field distribution, an iterative calculation may be required.

In this paper, the uniaxial magnetoelastic characteristics used in the numerical computation have been obtained using a simplified modeling approach detailed in [20]. Hysteresis effects are neglected. The saturation magnetization is  $0.8 \cdot 10^6$  A/m and the saturation magnetostriction strain is  $1640 \cdot 10^{-6}$ . The corresponding magnetization and magnetostriction curves are shown in Figs. 10 and 11, respectively. A good agreement is obtained compared to experimental measurements (see Fig. 7 and [16] and [21]). The modeling results in terms of permeability as a function of stress are shown in Fig. 12 for different magnetic field amplitudes.

## IV. APPLICATION

The calculation procedure has been implemented into the Matlab® environment. The studied configuration is detailed hereafter.

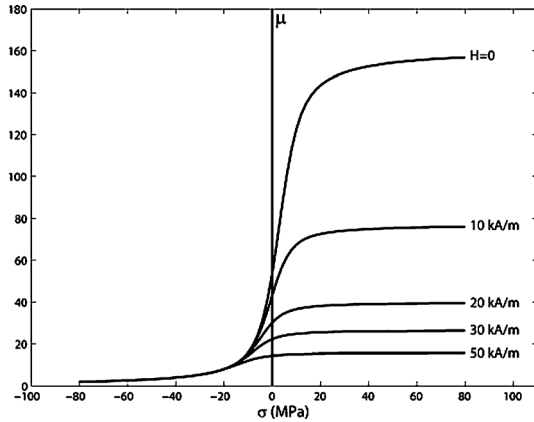


Fig. 12. Modeled stress-dependent magnetic permeability.

### A. Location of GMM Parts

In order to define the location of the GMM parts, the rotor of the PMSM is considered as a plain cylinder under inertial loading. Two configurations for the magnetic field in the GMM are investigated: radial or orthoradial. Plane geometry and plane strain are considered. The study is realized under quasi-static conditions.

The radial, orthoradial, and normal stress components  $\sigma_{rr}$ ,  $\sigma_{\theta\theta}$ , and  $\sigma_{zz}$  can then be expressed analytically:

$$\sigma_{rr} = \frac{3 - 2\nu}{8(1 - \nu)} \rho \omega^2 (R^2 - r^2) \quad (23)$$

$$\sigma_{\theta\theta} = \frac{1}{8(1 - \nu)} \rho \omega^2 ((3 - 2\nu)R^2 - (1 + 2\nu)r^2) \quad (24)$$

$$\sigma_{zz} = \frac{\nu}{4(1 - \nu)} \rho \omega^2 ((3 - 2\nu)R^2 - 2r^2). \quad (25)$$

$\nu$  is the Poisson's ratio of the material,  $\rho$  its mass density,  $\omega$  the rotation speed,  $R$  the external radius of the cylinder, and  $r$  the radius at the stress calculation position. The corresponding stress state as a function of the radius is plotted in Fig. 11 for  $\nu = 0.3$ . It must be noticed that this stress state is multiaxial.

The corresponding equivalent stress is calculated according to (15):  $\sigma_{eq}^r$  for a radial magnetic field ( $H/u_r$ ),  $\sigma_{eq}^o$  for an orthoradial magnetic field ( $H/u_\theta$ ). These equivalent stress values have also been reported in Fig. 13. Their expression is given by (26) and (27):

$$\sigma_{eq}^r = \frac{1 - 2\nu}{16(1 - \nu)} \rho \omega^2 ((3 - 2\nu)R^2 - 5r^2) \quad (26)$$

$$\sigma_{eq}^o = \frac{1 - 2\nu}{16(1 - \nu)} \rho \omega^2 ((3 - 2\nu)R^2 + r^2). \quad (27)$$

In the proposed PMSM structure, the GMM are tangentially oriented in order to have a positive equivalent stress. This positive stress will be added to the initial negative compression component. When the speed increases, the magnetic permeability is then increased as well (see Fig. 12). The initial compression stress can be chosen in order to control this inertial effect taking advantage of the nonlinear slope of the stress-permeability curve.

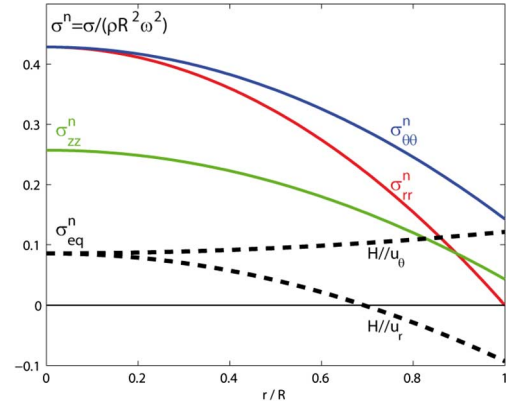


Fig. 13. Multiaxial stress state due to inertial forces and corresponding equivalent stresses.

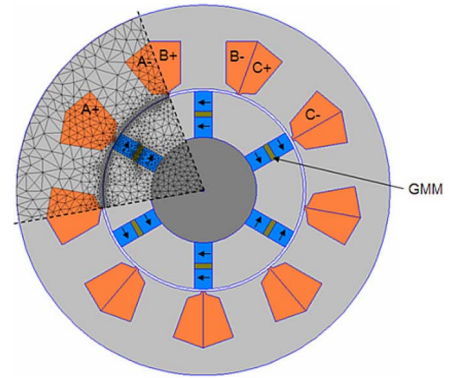


Fig. 14. Geometry and part of the mesh of the PMSM including giant magnetostrictive parts.

TABLE I  
PMSM SPECIFICATIONS

Stator outer diam. [mm]	137	Magnet Remanence [T]	0.3
Rotor outer diam. [mm]	73.4	Depth [mm]	120
GMM size [mm x mm]	6.5x2	Stator yoke [mm]	10
Magnet width [mm]	6.5	Polar opening [°]	50
Airgap [mm]	0.8	Tooth opening [°]	38

### B. Geometry

The considered structure is presented in Fig. 14. It is a three-phase machine with 9 teeth for 6 magnetic poles. The windings consist of concentrated coils. GMM parts are inserted between magnets. The main specifications of the PMSM are given in Table I.

### C. Simulation Conditions

The remanent flux density of the magnets has been chosen low to avoid the saturation of the GMM parts. The magnetic permeability of the stator and rotor is supposed to be linear. The magnetic permeability of Terfenol-D is both nonlinear and stress dependent according to Fig. 10.

The stress is calculated only in the rotor (shaft included). The contribution of magnetic forces to the elastic equilibrium is shown to be negligible [16]. They have not been taken into account in the source terms of the elastic problem. The contribution of magnetostriction strain to the stress level—through elastic incompatibilities—has been considered

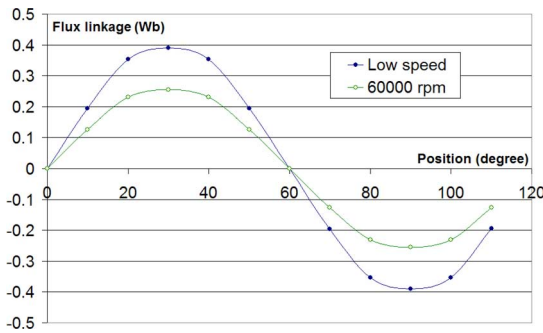


Fig. 15. Flux linkage for one coil calculated for two different speeds.

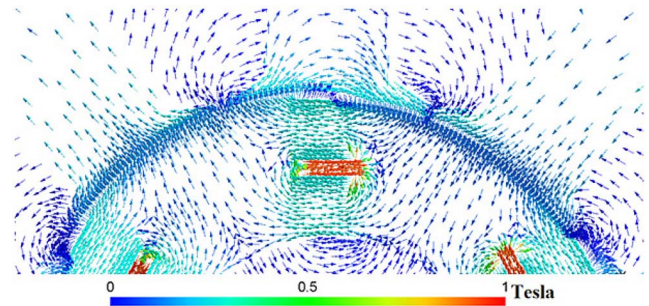


Fig. 18. Repartition of the magnetic flux density at high speed.

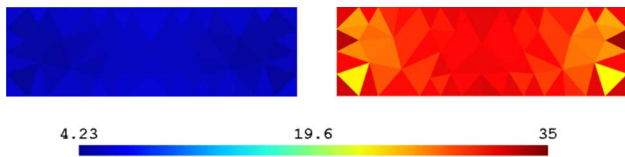


Fig. 16. Relative permeability in one GMM part for low and high speeds.

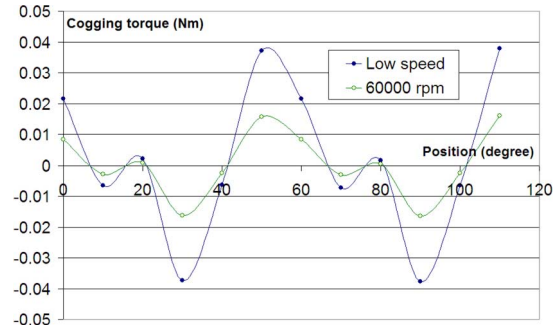


Fig. 19. Cogging torque for two different speeds.

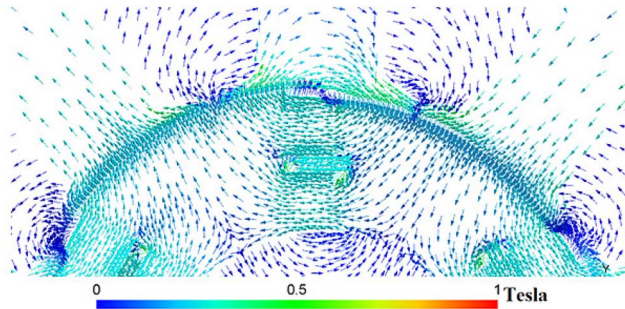


Fig. 17. Repartition of the magnetic flux density at low speed.

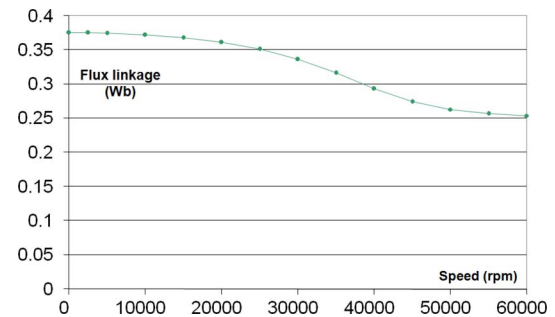


Fig. 20. Maximum of the flux linkage for one coil function of the speed.

as a second-order term compared to the effect of inertial stress. Including this contribution would need a more refined version of the simulation with the inclusion of the elastic FE calculation in the loop of Fig. 9. The centrifugal forces are assumed to play the central role in the stress distribution. The initial compressive stress applied to the GMM parts has been chosen as 30 MPa.

**D. Results**

At no load, the flux linkage of one coil has been computed for low (negligible centrifugal forces) and high speed (60 000 rpm), see Fig. 15. At high speed, the flux linkage is reduced by about 35%.

The relative permeability of a GMM part for the two speed levels is given in Fig. 16. The average value changes from 5.3 to 30.

The repartition of the magnetic field density (around a GMM part) for the two speed levels is given in Figs. 17 and 18. At high speed, an important part of the magnetic flux flows through the GMM.

The use of GMM also significantly reduces the cogging torque at high speed (about 50%); see Fig. 19. This can be an advantage regarding vibrations and noise.

The maximum of the flux linkage as a function of the speed is given in Fig. 20. At high speed, the curve tends to stabilize

because of the saturation of the GMM. The reduction of the flux linkage and consequently of the load torque are limited.

**V. CONCLUSION**

In this paper, a field weakening approach has been detailed for a permanent-magnet synchronous motor (PMSM). The principle is based on the use of giant magnetostrictive materials (GMM). GMM elements are inserted between the magnets in order to increase the magnetic leakages when the speed increases. Consequently, the flux linkages are reduced without additional power or mechanical devices. The proposed approach has been evaluated on a conventional motor structure with an original magnetoelastic calculation procedure. This procedure is based on the implementation of an equivalent stress for magnetoelastic behavior into a non linear magnetostatic finite element code. This procedure allows the investigation of the effect of multiaxial stress states on magnetoelastic behavior using standard finite element tools. The results at no load showed a reduction of the linkage flux

of about 35% for a rotation speed of 60 000 rpm compared to low speed figures. The cogging torque has also been shown to decrease at high speed.

The study has been limited to the case of permanent magnets with low remanence in order to avoid the saturation of GMM parts. Indeed, if GMM are saturated, the effect of stress on permeability decreases. The use of magnetostrictive materials with higher saturation magnetization would allow the use of standard magnets with remanence higher than 1 T. Additional investigations are to be performed in order to evaluate load torque, electromotive forces, or losses for such PMSM structures but the ability for field weakening has been demonstrated. The development of a prototype is part of an ongoing project and will be the subject of further publication.

#### REFERENCES

- [1] S. Morimoto, Y. Takeda, T. Hirasa, and K. Taniguchi, "Expansion of operating limits for permanent magnet motor by current vector control considering inverter capacity," *IEEE Trans. Ind. Appl.*, vol. 26, no. 5, Sep./Oct. 1990.
- [2] W. L. Soong and T. J. E. Miller, "Field-weakening performance of brushless synchronous AC motor drives," *IEE Proc. Elect. Power Appl.*, vol. 141, no. 6, Nov. 1994.
- [3] T. A. Lipo and M. Aydin, "Field weakening of permanent magnet machines—Design approaches," in *Int. Power Electronics & Motion Control Conf. (EPE-PEMC)*, Riga, Lettonia, Sep. 2004.
- [4] S. Hilioui, "Etude d'une machine synchrone à double excitation Contribution à la mise en place d'une plate-forme de logiciels en vue d'un dimensionnement optimal." (in French) Ph.D. thesis, Université de Technologie de Belfort-Montbéliard, France, Dec. 2008.
- [5] R. F. Schiferl and T. L. Lipo, "Power capability of salient pole permanent magnet synchronous motors in variable speed drive applications," *IEEE Trans. Ind. Appl.*, vol. 26, no. 1, pp. 115–123, Jan./Feb. 1990.
- [6] J. S. Hsu, "Direct control of air-gap flux in permanent-magnet machines," *IEEE Trans. Energy Convers.*, vol. 15, no. 4, pp. 361–365, Dec. 2000.
- [7] J. A. Tapia, F. Leonardi, and T. A. Lipo, "Consequent-pole permanent-magnet machine with extended field-weakening capability," *IEEE Trans. Ind. Appl.*, vol. 39, no. 6, pp. 1704–1709, Nov./Dec. 2003.
- [8] Y. Amara, J. Lucidarme, M. Gabsi, M. Lécrivain, A. Hamid Ben Ahmed, and A. D. Akémakou, "A new topology of hybrid synchronous machine," *IEEE Trans. Ind. Appl.*, vol. 37, no. 5, Sep./Oct. 2001.
- [9] J. F. Gieras and G. L. R. Ahmed, "Permanent Magnet Dynamoelectric Machine With Magnetic Flux Excitation," Patent US 2009/0251020, Hamilton Sundstrand Corp.
- [10] A. Shakal, Y. Liao, and T. A. Lipo, "A permanent magnet AC machine structure with true field weakening capability," in *IEEE Int. Symp. Industrial Electronics (ISIE)*, Budapest, Hungary, Jun. 1993.
- [11] K. Baoquan, L. Chunyan, and C. Shukang, "A new flux weakening method of permanent magnet synchronous machine," in *Electrical Machines and Systems Conf. (ICEMS)*, Nanjing, China, Sep. 2005.
- [12] F. Yoshiaki, "Rotor for Electric Rotating Machine," Patent JP2004343842A, Dec. 2, 2004, Denso Corp., inventor.
- [13] R. M. Bozorth, *Ferromagnetism*. New York: Van Nostrand, 1951.
- [14] E. du Trémolet de Lacheisserie, D. Gignoux, and M. Schlenker, Eds., *Magnetism: Fundamentals, Materials and Applications*. New York: Springer, 2002.
- [15] B. D. Cullity and C. D. Graham, *Introduction to Magnetic Materials*, 2nd ed. New York: Wiley, 2009.
- [16] N. Galopin, "Modélisation et caractérisation de matériaux actifs pour la conception de dispositifs magnéto-électriques," (in French) Ph.D. thesis, Université Paris-Sud 11, France, Dec. 2007.
- [17] W. Trowbridge and J. K. Sykulski, "Some key developments in computational electromagnetics and their attribution," *IEEE Trans. Magn.*, vol. 42, no. 4, pp. 503–508, Apr. 2006.
- [18] L. Daniel and O. Hubert, "Equivalent stress criteria for the effect of stress on magnetic behavior," *IEEE Trans. Magn.*, vol. 46, no. 8, pp. 3089–3092, Aug. 2010.
- [19] L. Daniel and O. Hubert, "An equivalent stress for the influence of multiaxial stress on the magnetic behavior," *J. Appl. Phys.*, vol. 105, p. 07A313, 2009.
- [20] L. Bernard, X. Mininger, L. Daniel, G. Krebs, F. Bouillault, and M. Gabsi, "Effect of stress on switched reluctance motors: A magneto-elastic finite element approach based on multiscale constitutive laws," *IEEE Trans. Magn.*, vol. 47, no. 9, pp. 2171–2178, Sep. 2011.
- [21] L. Daniel and N. Galopin, "A constitutive law for magnetostrictive materials and its application to Terfenol-D single and polycrystals," *Eur. Phys. J. Appl. Phys.*, vol. 42, pp. 153–159, 2008.